RSC Advances

ROYAL SOCIETY OF CHEMISTRY

www.rsc.org/advances

Cite this: DOI: 10.1039/c0xx00000x

www.rsc.org/xxxxxx

ARTICLE TYPE

Promotion of low-temperature oxidation of CO over Pd supported on titania-coated ceria

Atsushi Satsuma,[*,a,b] Masatoshi Yanagihara,[a] Kaoru Osaki,[a] Yurina Saeki,[a] Heng Liu,[a] Yuta Yamamoto,[c] Shigeo Arai,[c] and Junya Ohyama [a,b]

Received (in XXX, XXX) Xth XXXXXXXXX 20XX, Accepted Xth XXXXXXXXX 20XX
DOI: 10.1039/b000000x

A design of metal oxide support for Pd was investigated to promote the oxidation of CO at lower temperatures. Through a screening study using pure metal oxides, Pd/CeO_2 showed the highest activity above 100 ºC, while homemade TiO_2 was more effective below 100 ºC as a support for Pd. Applying the advantages of CeO_2 and TiO_2, we proposed a TiO_2/CeO_2 support having monolayer amount of surface TiO_2 supported on CeO_2. The $Pd/TiO_2/CeO_2$ catalyst showed higher activity than both Pd/TiO_2 and Pd/CeO_2 , which was not achieved by using CeO_2-TiO_2 mixed-oxide. The light-off temperature over $Pd/TiO_2/CeO_2$ was 100 ºC lower than Pd/Al_2O_3. The effect of surface TiO_2 was attributed to the promotion of reduction-oxidation cycle of supported Pd.

1. Introduction

In order to reduce carbon dioxide (CO_2) emissions from automobiles, better fuel economy systems, such as hybrid and start-stop systems, are becoming popular. The exhaust gas temperature of these systems is lower than ever because of the better energy efficiency. Hence, the enhancement of low-temperature activity is strongly required for automobile catalysts, especially for combustion of CO and unburned hydrocarbons as main components in the low-temperature exhausts.

Among platinum group metals (Pt, Pd, and Rh) as active elements in a three-way catalyst, a supported Pd catalyst is one of the essential components playing important role in the combustion of CO and unburned hydrocarbons. For the promotion of low-temperature activity of a supported Pd catalyst, we can find various strategies for catalyst design in the literature. Generally, the catalytic activity is correlated to the dispersion of supported Pd. For example, Baylet et al. reported that both higher surface area of supports and stability of Pd particles are required to achieve higher Pd dispersion on hexaaluminate.[1] The higher dispersion of Pd can be obtained by metal-support interaction under cycles between oxidative and reductive atmospheres encountered in an exhaust gas. Nishihata et al. developed so called "intelligent catalyst" based on Pd-loaded perovskite on which supported Pd retained its high metal dispersion by reversible incorporation of Pd^{n+} ions under oxidative atmosphere and formation of Pd^0 particles under reductive atmosphere.[2] The similar effect on the retention of metal dispersion is observed when CeO_2 and CeO_2-based supports are used as supports by forming solid solutions or the formation of metal-O-Ce bonds.[3,4]

The catalytic activity of supported Pd is sometimes more affected by the oxidation state of Pd. For example, we have reported very unique dependence of the oxidation activity of Pd/CeO_2 on surface area of the CeO_2 support, i.e., the lower surface area of CeO_2 was more preferable for the propene oxidation depending on the reaction and pre-treatment conditions.[5] In this case, the propane oxidation at 200 ºC proceeds preferably on metallic Pd species which is more stable in larger Pd particles on CeO_2 having low surface area. The metallic Pd species plays an important role on the oxidation reaction at lower temperatures, such as CO oxidation.[6,7] On the other hand, oxidized Pd species shows higher activity for the methane oxidation,[8-12] which is rationalized by the role of dispersed Pd oxide species as an oxygen provider.[13-15] The oxidation state of supported Pd is strongly affected by the acid-base property of supports.[3,10] It is also known that incorporated Pd species in metal oxide matrix shows activity for the oxidation reactions. Hedge and co-workers proposed "noble metal ionic catalysts" in the formulae of $Ce_{1-x}Pd_xO_{2-\delta}$ and $Ce_{1-x-y}Ti_yPd_xO_{2-\delta}$ (x = 0.01-0.02, $\delta \approx x$, y = 0.15-0.25) and $Ti_{1-x}Pd_xO_{2-x}$ (x = 0.01-0.03), which showed very high CO oxidation activity below 100 ºC.[16-21] Kuranatowska and co-workers also reported that nanocrystalline $Ce_{1-x}Pd_xO_{2-y}$ exhibited a good performance on the low-temperature CO oxidation.[22] In these catalysts, the low-temperature activity is assigned to the formation of Pd-O-Ce bond as a redox site and activation of lattice oxygen. Actually, Colussi et al. clearly demonstrated by means of HRTEM and DFT calculations that Pd-O sites in Pd-Ce surface enhanced the catalytic activity for methane combustion.[23]

As for the role of supports, oxygen storage and release capacity (abbreviated as OSC, hereafter) strongly controls the catalytic activity especially at lower temperatures. Liu et al. demonstrated an effective contribution of iron oxide support to low-temperature CO oxidation.[24] They reported that CO oxidation over Pt/FeOx and Pd/FeOx proceeds over two adjacent but different active sites (Pt, Pd for CO and FeOx for oxygen) with low apparent

activation energies (30–34 kJ/mol). Ikeue et al., reported that the use of partially Fe-substituted $10Al_2O_3 \cdot 2B_2O_3$ as a support of Pd gave an effective catalyst for the catalytic NO conversion in a fuel rich region because of improved oxygen storage capacity.[25] In the case of CeO_2-based supports, it is well known that partial incorporation of Zr and other elements in CeO_2 lattice significantly improves OSC.[26-31] Several papers demonstrated suitable designs of CeO_2-based metal oxide supports for promotion of CO oxidation activity using CeO_2,[32-34] CeO_2/Co_3O_4,[35-37] and CeO_2-TiO_2.[38-44] There are two major effects of CeO_2-based supports on the low temperature oxidation: One is the promotion of redox cycles of Pd particles, and another is supply of lattice oxygen.[7] As for the latter effect, the strong adsorption of CO on Pd surface strongly suppresses O_2 adsorption and activation on Pd particles in Pd/Al_2O_3 at lower temperatures, while CeO_2-based supports played a role of oxygen supply from lattice even when the Pd surface is fully covered by strongly adsorbed CO.[7]

On the basis of above mentioned activity-controlling factors for supported Pd catalysts, the present study aimed a design of novel supported Pd catalysts for low-temperature oxidation of CO. We focused TiO_2 having a limited promotion effect only at lower temperatures. Although mixed oxide of CeO_2-TiO_2 has been already proposed,[38-44] this study proposed hierarchical configuration of TiO_2 and CeO_2 for the better CO oxidation activity at lower temperatures.

2. Experimental section

Supported Pd catalysts with Pd content of 1 wt% were prepared by a conventional impregnation method using an aqueous palladium nitrate, followed by dryness and calcination in air at 500 ◦C for 3 h. CeO_2 (JRC-CEO-3), TiO_2(B) (JRC-TIO-8), ZrO2 (JRC-ZRO-1) were supplied from the committee of reference catalyst, Catalysis society of Japan. SiO_2 (Fuji Silysia, Q10) and Fe_2O_3 (Kishida Chemical, 98%) were purchased. Al_2O_3 was obtained by calcination of boehmite at 900 ºC in air for 3 h. TiO_2(A) was prepared by hydrolysis of $Ti(OC_3H_7)_4$ (Kishida Chemical, 99%) by an aqueous solution of ammonia followed by dryness and calcination in air at 500 ºC for 3 h. CeO_2-TiO_2 (Ce/Ti = 0.2) and TiO_2-ZrO_2 (Ti/Zr = 5/5) were prepared by co-precipitation[37-45] using $TiCl_4$ (Kishida Chemical, 24%), $Ce(NO_3)_4$ (Kishida Chemical, 98%) and $ZrO(NO_3)_2 \cdot 2H_2O$ (Kishida Chemical, 99%) as precursors. The mixed aqueous solutions were neutralized with an aqueous solution of ammonia (Kishida Chemical, 28%), and the obtained precipitates were dried and then calcined in air at 500 ºC for 3 h. TiO_2/CeO_2 supports were prepared by a precipitation method as follows. CeO_2 powder and distilled water were put in a beaker. After the temperature regulation of the beaker in a water bath, a prescribed amount of Ti source ($TiCl_4$ or $Ti(OC_3H_7)_4$) was added to the solution and stirred for 30 min. Then an aqueous solution of ammonia was added to adjust pH of the solution around pH = 8–9. The precipitates were filtrated and washed with distilled water, and then dried and calcined at 500 ºC for 3 h in air. The detailed preparation conditions are described in the section 3.2.

The catalytic activity was evaluated by CO oxidation using a conventional fixed-bed flow reactor at atmospheric pressure with a 10 mg of catalyst at a total flow rate of 100 N cm^3min^{-1} which corresponds to GHSV = 480,000 h^{-1}.[7] A catalyst was at first reduced in a flow of 3%H_2/He at 400 ºC for 10 min, and the catalytic run was carried out under a flow of 0.45% CO/10% O_2/N_2. The effluent gas was analyzed by nondispersive infrared (NDIR) CO/CO_2 analyzer (Horiba VIA510).

Temperature programmed reduction by CO (CO-TPR) was carried out using a conventional fixed-bed flow reactor as follows. The sample was oxidized in a flow of 20%O_2/N_2 (100 N cm^3min^{-1}) at 400 ºC for 30 min. After cooling the sample in a flow of pure N_2 to room temperature, the CO-TPR measurement was carried out in a flow of 0.4%CO/N_2 at a rate of 5 ºC min^{-1} up to 400 ºC. The effluent gas was analyzed by nondispersive infrared (NDIR) CO/CO_2 analyzer (Horiba VIA510).

The dispersion of Pd was estimated by the CO-pulse adsorption method.[46-48] A catalyst was at first treated in a flow of O_2 at 400 ◦C for 15 min followed by purge with He for 15 min, and then reduced in a flow of H_2 at 400 ºC for 15 min followed by purge with He for 15 min. Then the catalyst was cooled in a flow of He, and a series of CO pulses were injected with an interval of 2 to 3 min until the amount of slipped CO pulses reaches a steady state value. In order to avoid oxidation of CO to CO_2 followed by adsorption on CeO_2 as carbonate, the sample cell was soaked in a dry ice/ethanol bath and the adsorption of CO was carried out at ca. -70 ºC. The BET specific surface area was measured by N_2 adsorption at liquid N_2 temperature by using a conventional flow-type adsorption apparatus.

The oxygen storage-release property was evaluated by weight deviation under the following O_2–H_2 periodic operation at 300 ºC using TG-DTA(Shimadzu DTG-60H). In order to suppress the reduction-oxidation of supported Pd, the oxidation step was carried out under low oxygen concentration (3%). After pretreatment in a flow of 3%O_2/N_2 at 500 ºC for 30 min, the oxidized sample was cooled down to 300 ºC in 3%O_2/N_2. After purging with pure N_2 for 30 s, a flow gas was switched to 3%H_2/N_2 until the catalyst weight loss reaches to a steady state. Then the purging in pure N_2, oxidation in 3%O_2/N_2 until the catalyst weight recovered, the purging in pure N_2, and the reduction in 3%H_2/N_2 were repeated for several times at 300 ºC.

Pd K-edge XANES spectra were measured on BL28B2 of SPring-8 (Hyogo, Japan) operated at 8 GeV. The analyses of X-ray Absorption Near Edge Structure (XANES) were performed using the REX version 2.5 program (RIGAKU).

3. Results and Discussion

3.1. Screening study

At first, a screening study of the effect of support materials on the oxidation of CO was carried out as summarized in Table 1. The temperatures at which the CO conversion reached to 20% and 80% (T_{20} and T_{80}) were used as indexes of light-off and nearly complete oxidation, respectively. It should be noted that the results were reproducible as far as the activity tests were carried out below 500 ºC. The values of T_{20} for Pd catalysts supported on TiO_2, CeO_2, and CeO_2-based mixed oxides were below 100 ºC, while those were higher than 130 ºC when Al_2O_3, SiO_2, ZrO_2, and Fe_2O_3 were used as supports. As discussed in the previous paper,[7]

the reason for the high activity of Pd/CeO_2 and Pd/TiO_2 can be assigned to the promotion of reduction-oxidation cycles of supported Pd particles and the oxygen supply from the supports. It should be noted that the order of the activity was not dependent on the surface area or Pd dispersion. Although Pd dispersion of Pd/CeO_2 is less than a half of that of Pd/Al_2O_3, T_{20} of the former was 71 ºC lower than that of the latter. The lowest T_{20} (44 ºC) was obtained when homemade TiO_2(A) was used as a support. Interestingly, Pd/TiO_2(B) available in a market did not show such high activity at lower temperatures. The higher Pd dispersion on Pd/TiO_2(A) than Pd/TiO_2(B) is one of the possible reasons for the lowest T_{20}. However, T_{80} of both the Pd/TiO_2 was almost the same. The loss of the advantage of Pd/TiO_2(A) at higher temperature is not caused by sintering of Pd particles on Pd/TiO_2(A) because the activity patterns of all the catalysts were reproducible. The result suggests that the promotion effect is caused by an interaction between Pd and TiO_2(A), which is limited below 100 ºC. As shown in Fig. 1S, both the TiO_2 supports showed the diffraction lines of anatase phase, while the intensity of the diffraction lines of TiO_2(A) were significantly weaker than those of TiO_2(B). The result suggests major amorphous phase in TiO_2(A) may cause the promotive effect of CO oxidation at lower temperatures. In order to obtain more active catalyst, a design of a support is investigated using TiO_2 and CeO_2 in the next section.

Table 1. BET surface area (S_{BET}), dispersion of Pd (D_{Pd}), and temperatures at which CO conversions were 20% and 80% (T_{20} and T_{80}) for 1wt% Pd supported catalysts.

Catalysts	S_{BET} / m^2 g^{-1}	D_{Pd} / %	T_{20} /ºC	T_{80} /ºC
Pd/TiO_2 (A)	56	69	44	147
Pd/CeO_2	84	32	59	122
Pd/CeO_2-ZrO_2	36	12	71	168
Pd/TiO_2 (B)	130	23	84	151
Pd/CeO_2-TiO_2	200	35	88	138
Pd/Al_2O_3	242	71	130	176
Pd/SiO_2	414	16	149	<200
Pd/ZrO_2	11	10	155	195
Pd/Fe_2O_3	7.0	0.1	183	200

3.2. Design of TiO_2/CeO_2 support

Fig. 1 shows the activity patterns of Pd catalysts supported on CeO_2, TiO_2(A), and their mixed oxides. The activity pattern of Pd/Al_2O_3 was also plotted as a model of practical catalyst. Although the conversion of CO on Pd/TiO_2 is higher than Pd/CeO_2 below 110 ºC, the increase in CO conversion on Pd/TiO_2(A) slowed down above 100 ºC and became the same as Pd/Al_2O_3 above 180 ºC. Assuming that the mixing of CeO_2 and TiO_2 may result in a better performance, two types of supports were examined, i.e., CeO_2-TiO_2 mixed oxide[38-44] and TiO_2/CeO_2 supported oxide. The CO oxidation activity of Pd/CeO_2-TiO_2 (Ce/Ti = 0.2) was comparable to Pd/TiO_2 below 80 ºC, however, that was lower than Pd/CeO_2 above 110 ºC. On the other hand, after the optimization of chemical composition and preparation conditions, $Pd/TiO_2/CeO_2$ (TiO_2 =5.4wt%) showed the best activity from the light-off to the 100% conversion. The surface area and Pd dispersion of $Pd/TiO_2/CeO_2$ were 64 m^2g^{-1} and 35 %, respectively. Since the Pd dispersions of $Pd/TiO_2/CeO_2$ and Pd/CeO_2-TiO_2 are the same, the better activity of $Pd/TiO_2/CeO_2$ than Pd/CeO_2-TiO_2 is caused by another factor, as discussed in the section 3.3. Interestingly, the CO conversion over $Pd/TiO_2/CeO_2$-ZrO_2 (TiO_2 = 5.4wt%, Ce/Zr =5/5) did not exceed that of Pd/CeO_2 (Figure not shown). It should be noted that $Pd/TiO_2/CeO_2$ showed the CO oxidation activity around 100 ºC lower than Pd/Al_2O_3 which is a typical oxidation catalyst. The optimization of the chemical compositions and preparation conditions is reported below.

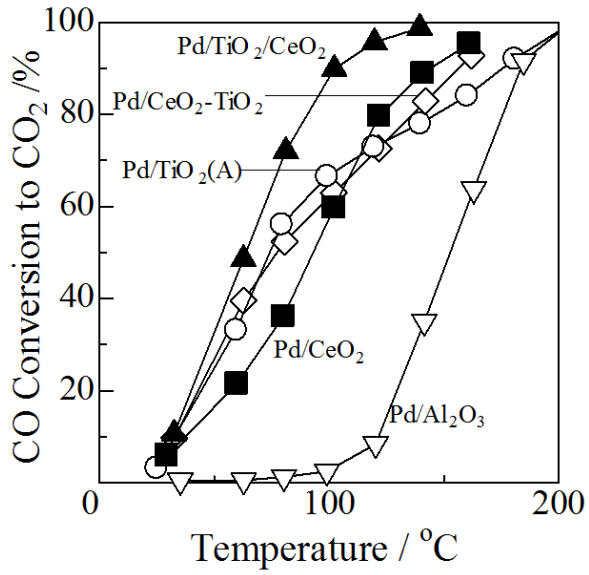

Fig. 1. Conversion of CO over 1wt% Pd supported catalysts.

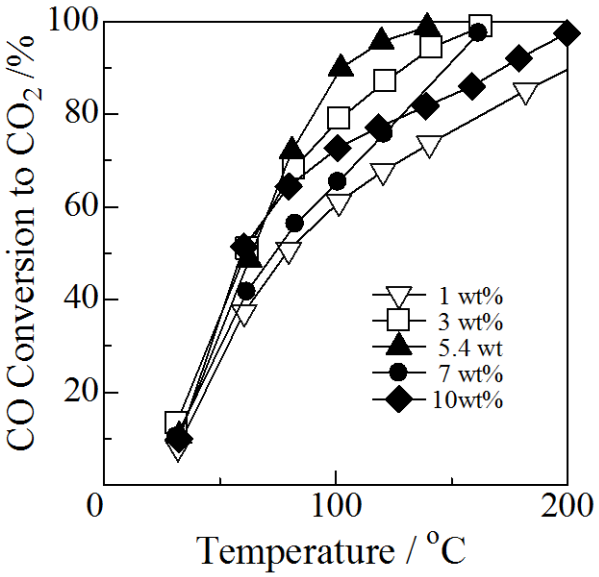

Fig. 2. Conversion of CO over $Pd/TiO_2/CeO_2$ having various TiO_2 contents.

Fig. 2 shows the effect of TiO_2 content on the CO oxidation activity of $Pd/TiO_2/CeO_2$. The catalytic activity increased with the increase in the TiO_2 content up to 5.4 wt%, and further

addition of TiO_2 suppressed the catalytic activity. It is interesting that the maximum activity was obtained when the theoretical amount of monolayer TiO_2 (5.4wt%) was supported on CeO_2.

Fig. 3 shows the effect of TiO_2 precursors and precipitation temperature on the CO oxidation activity of $Pd/TiO_2/CeO_2$. Using $TiCl_4$ as a precursor, the precipitation at 4 ºC (water/ice bath) resulted in the better catalytic performance than that precipitated at room temperature. The further decrease in the temperature to –20 ºC (NaCl/water/ice bath) was not effective. The use of $Ti(OC_3H_7)_4$ as a precursor was less effective than that of $TiCl_4$. The best catalyst performance was obtained when 5.4 wt% TiO_2 was precipitated to CeO_2 at 4 ºC using $TiCl_4$ as a precursor. The EDX images of the optimized support indicated uniform dispersion of TiO_2 on CeO_2 support, as shown in Fig. 2S. In the XRD pattern, there was no diffraction line assignable to TiO_2, indicating TiO_2 is in amorphous phase, very small particle, or thin layer. The promotion effect of TiO_2 layer on the CO oxidation suggests contacts between TiO_2 and Pd particles. The promotive role of surface TiO_2 is investigated in the next section.

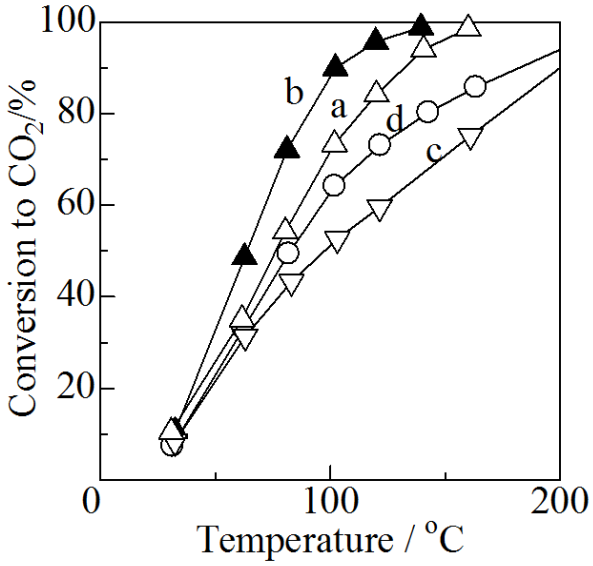

Fig. 3 Conversion of CO over $Pd/TiO_2/CeO_2$ catalysts. The TiO_2/CeO_2 supports were prepared using (a-c) $TiCl_4$, and (d) $Ti(OC_3H_7)_4$ as precursors and precipitated at (a) room temperature, (b) 4 ºC, (c) -20 ºC, and (d) 4 ºC.

3.3. Promotion effect of surface TiO_2 on CeO_2.

As discussed in the previous paper, the catalytic activity of supported Pd catalysts for the low temperature oxidation of CO can be rationalized by the following factors: (1) Reducibility of supported Pd species, (2) oxygen storage-release property of the supports, and (3) dispersion of Pd.[7] The factor (1) is essential for the activation of CO because coordinatively unsaturated surface sites of Pd metal particles are necessary for CO adsorption. The factor (2) is essential for the activation of O_2. Since the Pd dispersions of $Pd/TiO_2/CeO_2$, Pd/CeO_2, and Pd/CeO_2-TiO_2 were almost the same and lower than Pd/TiO_2, the factor (3) can be neglected as the reason for the best activity of $Pd/TiO_2/CeO_2$. Therefore, the factors (1) and (2) of $Pd/TiO_2/CeO_2$ are compared with Pd/CeO_2 and Pd/TiO_2.

The oxygen storage-release property was evaluated by weight deviation during the O_2–H_2 periodic operation at 300 ºC, and the results of Pd/TiO_2, Pd/CeO_2, and $Pd/TiO_2/CeO_2$ are shown in Fig. 4. It is clear that the maximum weight decrease is strongly dependent on the supports in the following order: $Pd/TiO_2/CeO_2$ (0.19 mmol-O_2 g^{-1}) ≥ Pd/CeO_2 (0.14 mmol-O_2 g^{-1}) >> Pd/TiO_2 (0.07 mmol-O_2 g^{-1}). The weight deviation of Pd/CeO_2 corresponds to the reduction of pure CeO_2 to $CeO_{2-\delta}$ (δ = 0.048), which is close to the maximum oxygen storage capacity for pure CeO_2 (δ =0.05).[27,29] On the other hand, the released oxygen from Pd/TiO_2 was only a half of that from Pd/CeO_2. The oxygen storage capacity of CeO_2 was retained after TiO_2 modification. The trend was the same at 200 ºC: The maximum weight decreases were $Pd/TiO_2/CeO_2$ (0.17 mmol-O_2 g^{-1}) ≥ Pd/CeO_2 (0.14 mmol-O_2 g^{-1}) >> Pd/TiO_2 (undetectable). The rates for oxygen release and storage at 300 ºC was estimated from the initial slope of the weight deviation, as shown in Fig. 3S. The estimated release rates were 0.54×10^{-6} mol-O_2 g^{-1} s^{-1} for Pd/TiO_2(A), and 1.8×10^{-6} mol-O_2 g^{-1} s^{-1} for Pd/CeO_2 and $Pd/TiO_2/CeO_2$. Pd/CeO_2 and $Pd/TiO_2/CeO_2$ showed 3.3 times faster rate than Pd/TiO_2(A). The oxygen storage rates of these three catalysts are the same (0.94×10^{-6} mol-O_2 g^{-1} s^{-1}). The results suggest the oxygen storage-release capacity and rate at 300 ºC of $Pd/TiO_2/CeO_2$ were comparable to Pd/CeO_2, indicating the contribution of OSC on higher CO conversion level. The lower activity of Pd/TiO_2(A) at higher temperatures can be rationalized by the lower oxygen storage capacity and release rate. Actually, above 180 ºC, Pd/TiO_2(A) showed comparable activity to Pd/Al_2O_3 having no oxygen storage capacity.

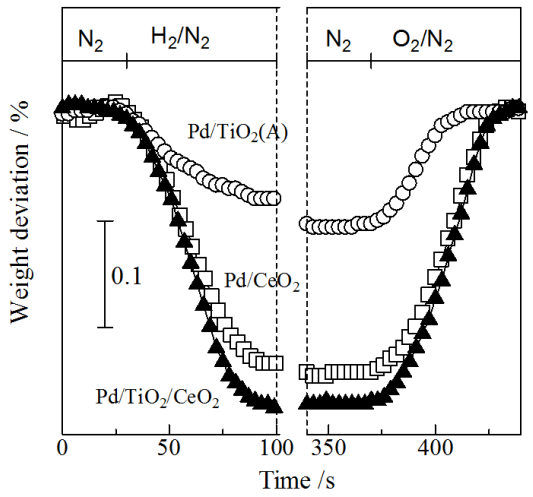

Fig. 4 Weight deviation of Pd/TiO_2, Pd/CeO_2, and $Pd/TiO_2/CeO_2$ during O_2–H_2 periodic operation at 300 ºC.

As discussed above, the contribution of OSC on CO oxidation above 100 ºC can be rationalized, but the contribution of OSC on the light-off activity cannot be discussed based on TG-DTA results because the weight deviation during the H_2-O_2 periodic operation was negligible below 100 ºC. Mukri and co-workers reported that $Ti_{1-x}Pd_xO_{2-x}$ prepared by substitution of TiO_2 by Pd^{2+} ion showed high catalytic activity for CO oxidation because of

activated lattice oxygen.[21] In their case, the formation Pd-O-Ti interface in lattice improved the catalytic activity due to high oxygen storage capacity up to 5.1 mmol g^{-1}, which was more than one order of magnitude higher than those for the catalysts in this study. Thus, the promotion effect of the TiO_2 layer cannot be attributed only to OSC enhancement. The different type of the effect of TiO_2 layer on Pd species can be expected. Therefore, reduction-oxidation property of the catalysts below 100 ºC was evaluated by CO-Temperature Programmed Reduction and in-situ XANES.

Fig. 5 shows CO-Temperature Programmed Reduction (CO-TPR) profiles of selected Pd supported catalysts. Before the TPR measurement, the supported Pd was oxidized to PdO, and the TPR measurement was carried out in 0.4%CO/N_2 without O_2. Pd/Al_2O_3 showed a reduction peak around 165 ºC. The amount of evolved CO_2 (0.11 mmol g^{-1}) in the first peak was almost equivalent to the stoichiometry of PdO reduction to Pd (0.094 mmol g^{-1}). The other catalysts showed two reduction peaks below 150 ºC and above 150 ºC. As for the first peak, the amount of evolved CO_2 (0.13 mmol g^{-1} for Pd/TiO_2, 0.37 mmol g^{-1} for Pd/CeO_2, and 0.40 mmol g^{-1} for Pd/TiO_2/CeO_2, respectively) was higher than the stoichiometry of the PdO reduction to metallic Pd. The excess formation of CO_2 is caused by the oxygen release from the supports.[7] The reduction peak above 150 ºC is attributed to the contribution of supports or disproportionation of CO. The maximum reduction temperature of the first peak was in the order of Pd/TiO_2/CeO_2 (78 ºC) < Pd/CeO_2 (96 ºC) < Pd/TiO_2 (113 ºC) << Pd/Al_2O_3 (165 ºC). This order was not well in harmony with that of CO oxidation activity, because the reduction temperature of Pd/TiO_2 was higher than Pd/CeO_2 and the positions of the first peak of Pd/TiO_2/CeO_2 and Pd/CeO_2 are too close on both temperature and quantity to attribute the big difference in the CO conversion at 60 ºC for these catalysts (21% for Pd/CeO_2 and 48% for Pd/TiO_2/CeO_2, respectively). From the results of CO-TPR, we cannot conclude that the catalytic activity is controlled by the reducibility of supported Pd species from PdOx to Pd or OSC. Then, to investigate the oxidation step of supported Pd particles (from Pd to PdOx), in-situ XANES spectra are compared.

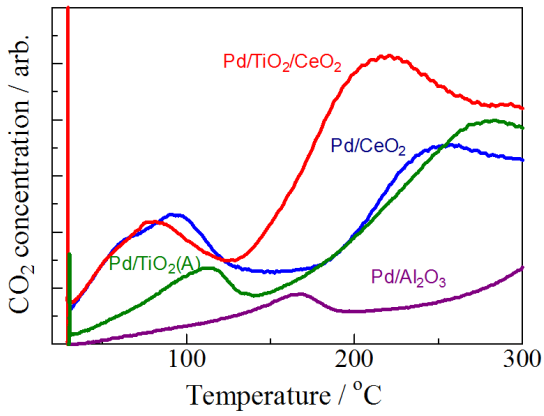

Fig. 5 Effluent CO_2 profile during CO-Temperature Programmed Reduction of supported Pd catalysts.

Fig. 6 shows in-situ Pd K-edge XANES spectra of supported Pd catalysts under the CO oxidation conditions below 100 ºC. The feed gas compositions are the same as in the catalytic tests. Under the CO oxidation, the spectra of supported Pd catalysts are similar to that after the reduction in H_2, indicating the supported Pd species is basically in metallic state. However, the shift of the absorption edge to the higher energy suggests certain contribution of oxidized Pd species. The oxidation state of Pd was evaluated in the following manner. Because of the interaction between Pd species and supports, the spectra were not reproduced by the combination of the spectra of pure PdO disk and Pd foil. Therefore, we used the spectra of catalysts after calcination as a reference of oxidized state (Ox. in the figures) and after reduction in H_2 at 400 ºC as a reference of reduced state (Red. in the figures). The measured in-situ XANES spectra were well reproduced by the combination of these reference spectra. Table 2 shows the evaluated contribution of oxidized Pd under the CO oxidation. The oxidation state of Pd was strongly affected by the supports. The contribution of oxidized Pd was less than 10% on Pd/Al_2O_3 which was not active for the CO oxidation below 100 ºC. On the other hand, more than 10% of Pd is oxidized on TiO_2/CeO_2 and TiO_2 supports even at room temperature. With the increase in the reaction temperature, the oxidation number of Pd increased for all the catalysts. Although the contribution of oxidized Pd in Pd/CeO_2 was lower than that of Pd/TiO_2/CeO_2 below 50 ºC, they were almost the same at 100 ºC. As for Pd/TiO_2, the contribution of oxidized Pd was comparable to that of Pd/TiO_2/CeO_2 at room temperature, while that was not sensitive to reaction temperature. The trend in the oxidation state of Pd is in harmony with the CO oxidation activity. The results in the table suggest contribution of the oxidation step of Pd under the CO oxidation as an activity-controlling factor.

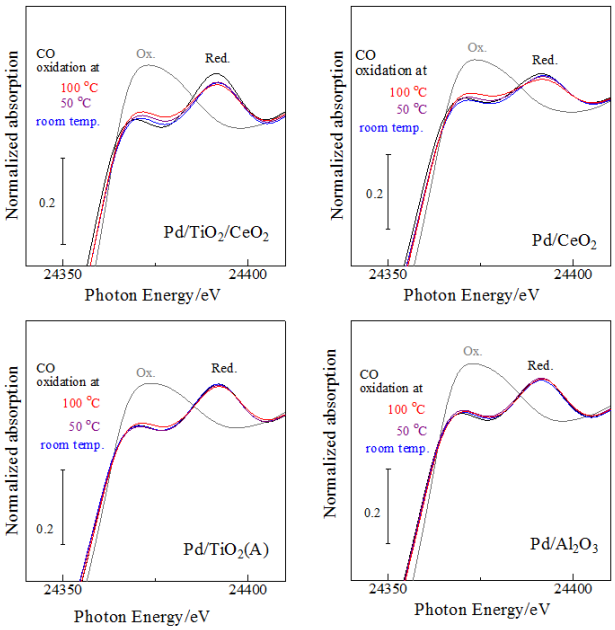

Fig. 6 Pd K-edge XANES spectra of supported Pd catalysts (Ox.) after calcination at 500 ºC. in air, (Red.) after reduction in H_2 at 400 ºC for 30 min, and in-situ Pd K-edge XANES spectra under the CO oxidation at various temperatures.

Table 2. Contribution of oxidized Pd in Pd particles (% in total Pd) under the CO oxidation at various temperatures evaluated from in-situ XANES spectra.

Catalyst	Room temp.	50 ºC	100 ºC
$Pd/TiO_2/CeO_2$	16.2	18.9	23.6
Pd/CeO_2	7.4	13.7	23.7
Pd/TiO_2(A)	10.7	13.1	16.9
Pd/Al_2O_3	4.0	4.7	6.8

One may wonder above discussion: Although the reducibility of Pd is one of the activity-controlling factors, the promotion effect of TiO_2 modification was attributed to the rate of oxidation of Pd. The results can be rationalized by considering the reduction-oxidation cycle of Pd species during the CO oxidation. The oxidation of CO over Pd catalyst can be generally depicted in the following scheme.

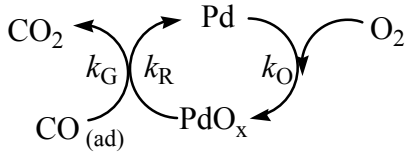

In lean conditions (oxygen-rich atmospheres), Pd species are partially oxidized by gaseous oxygen or oxygen from supports. The oxidation of CO proceeds with the reduction of PdOx to metallic Pd. The rates for both Pd oxidation (k_O) and PdOx reduction (k_R) determine the activity of gas phase CO oxidation (k_G). Comparing $Pd/TiO_2/CeO_2$ and Pd/CeO_2, the rates of PdOx reduction to Pd (k_R) by CO are not much different because the reduction peaks in CO-TPR were observed at the same temperature range. It suggests that the rate determining step is the regeneration of PdOx species (k_O). Although the rate of PdOx regeneration cannot be evaluated, the oxidation state under the reaction conditions estimated by XANES spectra indicates the equilibrium constant ($K = k_O/k_R$) under the reaction conditions. The contribution of PdOx under the reaction conditions should indicate the relative difference of K in each sample, and Pd species on $Pd/TiO_2/CeO_2$ is more easily oxidized than that on Pd/CeO_2 at lower temperatures. The results indicate that the promotive effect of TiO_2 can be attributed to the promotion of the regeneration step of oxidized PdOx species. The promotive effect was limited at lower temperatures, i.e., contributions of oxidized Pd were much higher on $Pd/TiO_2/CeO_2$ and Pd/TiO_2, while at 100 ◦C that of Pd/CeO_2 became almost the same as $Pd/TiO_2/CeO_2$ but Pd/TiO_2 showed lower value. The variation in the PdOx ratio as a function of reaction temperature is approximately in harmony with the activity pattern for CO oxidation shown in Fig. 1. Therefore, it is reasonable to attribute the promotive effect of TiO_2 modification to the promotion of re-oxidation step of Pd species under the CO oxidation.

Conclusions

The effect of metal oxide support was investigated to promote the CO oxidation over supported Pd catalysts at lower temperatures. The use of TiO_2 support enhanced the CO oxidation below 100 ◦C, and that of CeO_2 support was effective above 100 ºC. Applying the advantages of CeO_2 and TiO_2, $Pd/TiO_2/CeO_2$ showed the best catalytic activity from the light-off to the 100% conversion, which was around 100 ºC lower than Pd/Al_2O_3. After the optimization of the chemical compositions and preparation conditions, the best catalyst performance was obtained when theoretical monolayer amount (5.4 wt%) of TiO_2 was precipitated to CeO_2 at 4 ºC using $TiCl_4$ as a precursor. By using TG-DTA, CO-TPR, and in-situ XANES, the promotion of the oxidation step of Pd species during the CO oxidation was revealed to be an activity-controlling factor.

Acknowledgements

This work was partly supported by JSPS KAKENHI Grant from the Ministry of Education, Culture, Sports, Science and Technology, Japan. A part of this work was performed under a management of "Elements Strategy Initiative for Catalysts & Batteries (ESICB) " supported by MEXT program "Elements Strategy Initiative to Form Core Research Centre" (since 2012), MEXT; Ministry of Education Culture, Sports, Science and Technology, Japan. The XAFS measurements at SPring-8 were carried out by the approval (proposal no. 2012B1569) of the Japan Synchrotron Radiation Research Institute (JASRI).

Notes and references

[a] *Graduate School of Engineering, Nagoya University, Nagoya 464-8603, Japan. FAX: +81-52-789-3193; Tel: +81-52-789-4608; E-mail: satsuma@apchem.nagoya-u.ac.jp*
[b] *Unit of Elements Strategy Initiative for Catalysts & Batteries, Kyoto University, Kyoto 615-8530, Japan.*
[c] *Ecotopia Science Institute, Nagoya University, Nagoya, 464-8603*

† Electronic Supplementary Information (ESI) available: XRX patterns of Pd supported catalysts, TEM/EDS micrographs of TiO_2/CeO_2 support, and the estimation of oxygen storage-release rate from TG-DTA. See DOI: 10.1039/b000000x/

1 A. Baylet, S. Royer, P. Marecot, J.M. Tatibouet, D. Duprez, *Appl. Catal.s B: Environ.*, 2008, **77**, 237-247.
2 Y. Nishihata, J. Mizuki, T. Akao, H. Tanaka, M. Uenishi, M. Kimura, T. Okamoto, N. Hamada, *Nature*, 2002, **418**, 164-167.
3 Y. Nagai, T. Hirabayashi, K. Dohmae, N. Takagi, T. Minami, H. Shinjoh, S. Matsumoto, *J. Catal.*, 2006, **242**, 103-109.
4 R.V. Gulyaev, A.I. Stadnichenko, E.M. Slavinskaya, A.S. Ivanova, S.V. Koscheev, A.I. Boronin, *Appl. Catal. A:Gen*, 2012, **439–440**, 41–50.
5 A. Satsuma, R. Sato, K. Osaki, K. Shimizu, *Catal. Today*, 2012, **185**, 61-65.
6 K.B. Kim, M.K. Kim, Y.H. Kim, K.S. Song, E.D. Park, *Res. Chem. Intermed.*, 2010, **36**, 603-611.
7 A. Satsuma, K. Osaki, M. Yanagihara, J. Ohyama, K. Shimizu, *Appl. Catal. B: Environ.*, 2013, **132-133**, 511-518.
8 R.F. Hicks, H. Qi, M.L. Young, R.G. Lee, *J. Catal.*, 1990, **122**, 295–306.
9 R. Burch, P.K. Loader, F.J. Urbano, *Catal. Today*, 1996, **27**, 243–248.
10 H. Yoshida, T. Nakajima, Y. Yazawa, T. Hattori, *Appl. Catal. B: Environ.*, 2007, **71**, 70–79.
11 P. Castellazzi, G. Groppi, P. Forzatti, E. Finocchio, G. Busca, *J. Catal.*, 2010, **275**, 218–227.
12 S. Colussi, A. Trovarelli, E. Vesselli, A. Baraldi, G. Comelli, G. Groppi, J. Llorca, *Appl. Catal. A: Gen.*, 2010, **390**, 1–10.
13 T. Schalow, B. Brandt, M. Laurin, S. Schauermann, S. Guimond, H. Kuhlenbeck, J. Libuda, H.-J. Freund, *Surf. Sci.*, 2006, **600**, 2528–2542.

14 S. Specchia, E. Finocchio, G. Busc, P. Palmisano, V. Specchia, *J. Catal.*, 2009, **263**, 134–145.
15 S. Specchia, E. Finocchio, G. Busca, G. Saracco, V. Specchia, *Catal. Today*, 2009, **143**, 86–93.
16 M.S. Hedge, G. Madras, K.C. Patil, *Acc. Chem. Res.*, 2009, **42**, 704-712.
17 P. Bera, A. Gayen, M.S. Hedge, N.P. Lalla, L. Spadaro, F. Fursteri, F. Arena, *J. Phys. Chem. B*, 2003, **107**, 6122-6130.
18 T. Baidya, A. Gayen, M.S. Hegde, N. Ravishankar, L. Dupont, *J. Phys. Chem. B*, 2006, **110**, 5262–5267.
19 T. Baidya, M.S. Hegde, N. Ravishankar, A. Marimuthu, G. Madras, *J. Phys. Chem.C*, 2007, **111**, 830–839.
20 T. Baidya, G. Dutta, M.S. Hegde, U.V. Waghmare, *Dalton Trans.*, 2009, **455**, 455-464.
21 B.D. Mukri, G. Dutta, U.V. Waghmare, M.S. Hegde, Chem. Mater. 2012, 24, 4491-4502.
22 M. Kurnatowska, L. Kepinski, W. Mista, *Appl. Catal. B: Environ.*, 2012, **117-118**, 135-147.
23 S. Colussi, A. Gayen, M.F. Camellone, M. Boaro, J. Llorca, S. Fabis, A. Trovarelli, *Angew. Chem. Int. Ed.*, 2009, **48**, 8481-8484.
24 L. Liu, F. Zhou, L. Wang, X. Qi, F. Shi, Y. Deng, *J. Catal.*, 2010, **274**, 1–10.
25 K. Ikeue, K. Watanabe, T. Minekishi, A. Imamura, T. Sato, Y. Nagao, Y. Nakahara, M. Machida, *Appl. Catal. B: Environ.*, 2014, **146**, 50–56.
26 H.C. Yao, F.Y. Yao, *J. Catal.*, 1984, **86**, 254–265.
27 M. Ozawa, M. Kimura, A. Isogai, *J. Alloys Compd.*, 1993, **193**, 73–75.
28 M. Sugiura, M. Ozawa, A. Suda, T. Suzuki, T. Kanazawa, *Bull. Chem. Soc. Jpn.*, 2005, **78**, 752–767.
29 G. Dutta, U. Vagmare, T. Baidya, M.S. Hegde, K.R. Priolkar, P.R. Sarode, *Catal. Lett.*, 2006, **108**, 165–172.
30 G. Dutta, U. Vaghmare, T. Baidya, M.S. Hegde, K.R. Priolkar, P.R. Sarode, *Chem. Mater.*, 2006, **18**, 3249–3256.
31 Q. Ding, S. Yin, C. Guo, T. Sato, *Chem. Lett.*, 2012, **41**, 1250-1252.
32 T. Jin, T. Okuhara, G.J. Mains, J.M. White, *J. Phys. Chem.*, 1987, **91**, 3310–3315.
33 G.S. Zafiris, R.J. Gorte, *J. Catal.*, 1993, **139**, 561–567.
34 H. Cordatos, R.J. Gorte, *J. Catal.*, 1996, **159**, 112–118.
35 J.-Y. Luo, M. Meng, X. Li, X.-G. Li, Y.-Q. Zha, T.-D. Hu, Y.-N. Xie, J. Zhang, *J. Catal.*, 2008, **254**, 310–324.
36 A. Tömcrona, M. Skoglundh, P. Thormählen, E. Fridell, E. Jobson, *Appl. Catal. B: Environ.*, 1997, **14**, 131–146.
37 A. Martínez-Arias, M. Fernández-García, A. Iglesias-Juez, A.B. Hungría, J.A. Anderson, J.C. Conesa, J. Soria, *Appl. Catal. B: Environ.*, 2001, **31**, 39–50.
38 G. Dong, J. Wang, Y. Gao, S. Chen, *Catal. Lett.*, 1999, **58**, 37-41.
39 H. Zhu, Z. Qin, W. Shan, W. Shen, J. Wang, *J. Catal.*, 2004, **225**, 267-277.
40 H. Zhu, Z. Qin, W. Shan, W. Shen, J. Wang, *J. Catal.*, 2005, **233**, 41–50.
41 H. Zhu, Z. Qin, W. Shan, W. Shen, J. Wang, *Catal. Today*, 2007, **126**, 382-386.
42 S. Yang, W. Zhu, Z. Jiang, Z. Chen, J. Wang, *Appl. Surf. Sci.*, 2006, **252**, 8499–8505.
43 F. Liang, H. Zhu, Z. Qin, G. Wang, J. Wang, *Catal. Commun.*, 2009, **10**, 737–740.
44 K. Nakagawa, Y. Murata, M. Kishida, M. Adachim, M. Hiro, K. Susa, *Mater. Chem. Phys.*, 2007, **104**, 30–39.
45 H. Zou, Y.S. Lin, *Appl. Catal. A:Gen.*, 2004, **265**, 35–42.
46 T. Tanabe, Y. Nagai, T. Hirabayashi, N. Takagi, K. Dohmae, N. Takahashi, S. Matsumoto, H. Shinjoh, J.N. Kondo, J.C. Schouten, H.H. Brongersma, *Appl. Catal. A: Gen.*, 2009, **370**, 108–113.
47 K. Shimizu, Y. Saito, T. Nobukawa, N. Miyoshi, A. Satsuma, *Catal. Today*, 2008, **139**, 24–28.
48 K. Shimizu, Y. Saito, T. Nobukawa, A. Satsuma, *Top. Catal.*, 2010, **53**, 584–590.